Effect of Cathode Contacting on Anode Supported Cell Performances

R. Spotorno[a], P. Piccardo[a], G. Schiller[b]

[a] Department of Chemistry and Industrial Chemistry, University of Genoa, Genoa, Italy
[b] German Aerospace Center (DLR), Stuttgart, Germany

The contact geometry effect on anode-supported cells (ASCs) performances has been evaluated by means of current-voltage curves (I-V curves) and electrochemical impedance spectroscopy (EIS). The use of platinum meshes and Crofer 22 APU interconnects as current collectors has been compared. Additionally, the application of $La_{0.6}Sr_{0.4}Co_{0.2}Fe_{0.8}O_3$ (LSCF) as contacting paste between the electrode and the metallic current collector allowed to estimate its beneficial effect by enhancing the current distribution at the cathode side. An inverse proportionality between the ohmic contributions and the extension of the contacting area has been observed. The usage of a contacting layer positively affected the polarization contribution as well. Both effects influenced positively the cell performances. The reduction of the ohmic losses resulted in a higher impact on the power density.

Introduction

Stacking Solid Oxide Fuel Cells implies the use of contacting layers, especially in the cathodic compartments. Here the high interfacial resistance and the lowered contact area caused by geometrical and porosity issues (1-3) may give rise to ohmic losses at the interface between the electrode and the interconnect. Such losses affect the current distribution over the electrodes strongly influencing the system performances in terms of power output. Whereas the cell polarization losses depend by the current load on the cell (4), the contacting issues are poorly affected by the operating conditions and have to be faced at the structural level, this in order to ensure high stack performances (4, 5). The application of a contacting layer between the cathode and the current collector (i.e. platinum mesh or steel interconnect) enhances the electrical contact and improves the planar conductivity over the cathode area (6).

The application of a conductive interlayer in a power system mitigates the losses and allows a better characterization of its components since the current distribution can significantly influence the results of the electrochemical analyses. In this study a dedicated setup was used to test commercial ASCs with different contacting solutions. The performances of the system ASC-Interconnect with or without the contacting interlayer were studied by means of I-V curves. EIS measurements were carried out to distinguish the loss contributions within the system. The cells were then characterized post-experiment by scanning electron microscopy (SEM) equipped with energy dispersive X-ray spectroscopy (EDX) in order to correlate microstructural features with the observed performances.

Materials and methods

In this study the following materials were used in various combinations:

- Commercially available ASCs manufactured by CeramTec AG (Marktredwitz, Germany) were tested with and without contacting paste at the cathode side, using different metal current collectors. Such cells consisted of a 50 mm x 50 mm Ni/8YSZ-cermet anode (where 8YSZ: 8 mol% Y_2O_3 doped ZrO_2), a 50 mm x 50 mm 8YSZ electrolyte with GDC ($Ce_{0.8}Gd_{0.2}O_{2-\delta}$) interlayer at the cathode side followed by a LSCF ($La_{0.6}Sr_{0.4}Co_{0.2}Fe_{0.8}O_{3-\delta}$) 40 mm x 40 mm cathode (Figure 1).
- Commercially available LSCF powder (FCM, USA) was mixed with a solvent blend (94 wt.% terpineol, 6 wt.% polyethylene glycol) to form an ink (60 wt.% powder, 40 wt.% solvent) used as contacting paste to be applied on the ASC cathode. Such mixture was homogenized in an Exakt 80E three roll mill (Exakt Advanced Technologies GmbH, Norderstedt, Germany). The LSCF ink was brushed over the cathode to obtain a homogeneous layer.
- Metallic meshes (Heraeus Deutschland GmbH & Co. KG) with a wire diameter of 0.04 mm, mesh width of 0.12 mm and 3600 meshes per cm^2 were used as current collector between the cell and the electronic characterization devices at both the anode and the cathode side. On both sides Pt meshes were spot-welded with the platinum wires used as potential probes and current carriers. Between these meshes and the electrodes were placed a platinum mesh at the cathode side and a nickel one at the anode. The use of a Ni mesh at the anode was intended to avoid alloying between the platinum contacts and the nickel contained in the electrode (7).
- Crofer 22 APU plates 0.5 mm thick (ThyssenKrupp VD) were shaped by a stamping process (Graebner Maschinentechnik GmbH & Co. KG, Germany) to obtain metallic interconnects. The interconnects were squared corrugated 30 mm x 30 mm plates characterized by an asymmetric design with 3.5 mm wide air channels and 0.5 mm wide contact ribs.

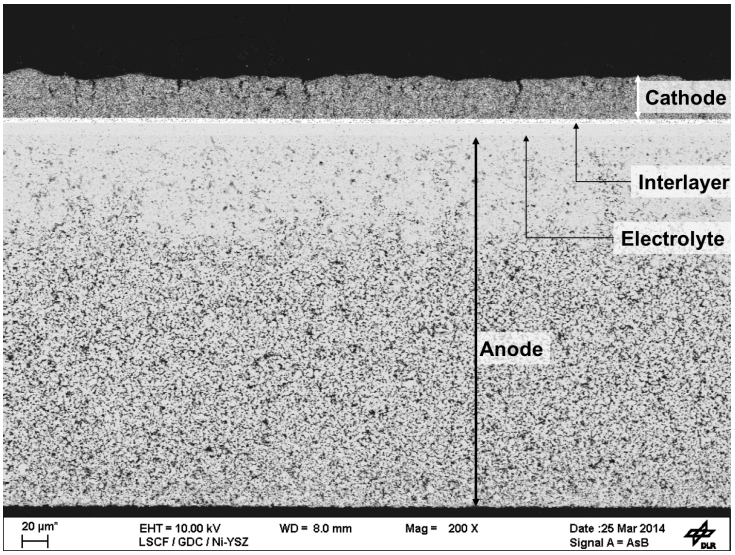

Figure 1. SEM-BSE image of an ASC cross-section.

The system ASC-Interconnect was tested using a dedicated sample holder designed on purpose and manufactured in Macor® (SiO_2 46 wt.%, MgO 17 wt.%, Al_2O_3 16 wt.%, K_2O 10 wt.%, B_2O_3 7 wt.%, F 4 wt.%) (Figure 2). This sample holder can host a 50 mm x 50 mm ASC and includes channels for the gas feeding and distribution at the electrodes.

An additional part of the sample holder at the cathode side was designed to host the metallic interconnect in contact with the cathode. The goal was to reproduce the electrode-interconnect interface in order to test their interaction and the behaviour of the cell with different contacting solutions. A modification of the gas distributor geometry allowed to force the gas flow through the interconnect channels limiting leakages.

Two configurations were tested: one using Pt meshes only and one using the interconnect between the cathode and the Pt meshes. In both cases the electrical wiring was spot-welded to the platinum meshes.

Weights (arrows in Figure 2) were placed on top of the cell housing to enhance the electrical contacting and the sealing between the two gas compartments, which was achieved using a gold gasket. In this study, 1500 g were applied on the cathode head obtaining a mechanical load of 9200 Pa on the contacted cathode area. 1400 g were placed on the sealing frame, which compressed the gold gasket ensuring gas tightness between the cathode and the anode compartment. Such sealing method was implemented in order to avoid the use of glass sealants and thus obtaining some advantages as a better experiment reproducibility and ease to set up.

The cell housing was mounted in a furnace capable to heat up to 1000°C and provided with gas and wiring ducts.

Thermocouples were located in the furnace environment and in the cell housing using proper grooves and thus allowing to monitor the cell temperatures in specific parts (i.e. cathode side, anode side, fuel inlet/outlet, oxidant inlet/outlet) to detect possible combustion of the fuel due to unwanted leakages through the sealant or ceramic components.

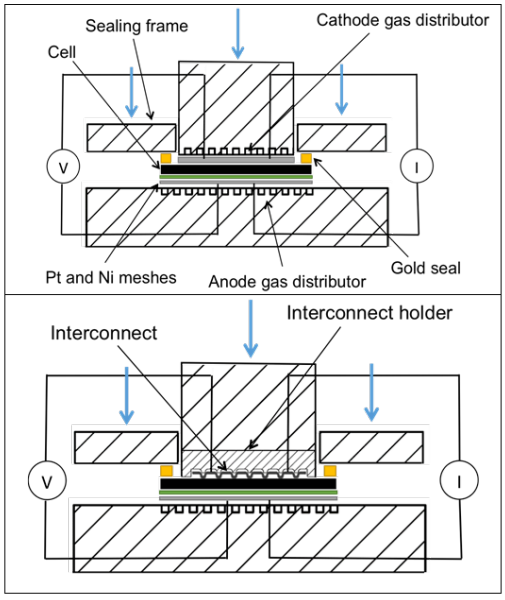

Figure 2. Scheme of testing setup with ceramic gas distributors (above) and with metallic interconnect as gas distributor/current collector on the cathode side (below).

Each cell was heated up to 900°C under a dry air flow at the cathode side (0.5 Nl min^{-1}) and dry nitrogen at the anode side (0.5 Nl min^{-1}). The heating speed was 5°C min^{-1} to avoid excessive thermal shocks of the cell and the ceramic cell housing. At 900°C the reduction of the anode was performed through step-wise increase of the hydrogen concentration in the anode gas flow (8, 9). The gas feeding to the electrodes was turned in five steps to 1 Nl min^{-1} of 3% wet hydrogen at the anode and 1 Nl min^{-1} of air at the cathode resulting in negligible fuel utilization during the whole testing procedure.

The furnace temperature was reduced to 750°C and the cell performances were evaluated by I-V curves and EIS measurements. The electrical characterization was carried out using an Electrochemical Workstation IM6 (Zahner-Elektrik GmbH & Co. KG, Kronach, Germany) in a frequency range of 0.1 Hz-100 kHz.

A priori hypothesis about the system functioning to build the model were found in literature from studies on analogous ASCs by means of analysis of the Distribution of Relaxation Times (10-13). In Figure 3 the equivalent circuit adopted in this study for the CNRLS fitting is shown.

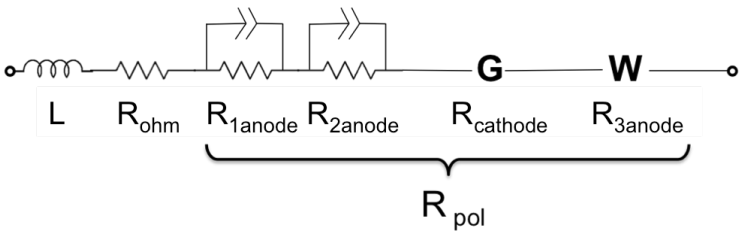

Figure 3. Equivalent circuit adopted for CNRLS fitting.

The ohmic losses, due to the resistances of the electrolyte and the contacting were described by the resistor named R_{ohm}. Its value is detectable in the EIS spectrum as the high-frequency intercept with the real part axis. Two RQ elements (R_{1anode} and R_{2anode}) at the higher frequencies of the cell polarization were used to describe the anodic losses in the anode functional layer related to the gas diffusion, charge transfer and ionic transport in the bulk of the electrode. A bounded Warburg element (R_{3anode}) described the gas diffusion impedance of the anode substrate. A Gerischer element corresponded to the cathode contribution including the oxygen surface exchange kinetics and the oxygen ions diffusivity within the electrode bulk. The inductance contribution, mainly due to the wiring providing the connection between the cell and the instrument, was modelled by an inductive element. Fitting was performed by Complex Non-Linear Regression Least-Squares (CNRLS) (14-17) using the software Thales-SIM (Zahner-Elektrik GmbH & Co. KG, Kronach, Germany) accepting a fitting error below 1% and relative uncertainty of each element lower than 30%.

After each test, the cell and interconnect were separated and individually studied. Cross-sections of samples were prepared by mounting in epoxy resin, cutting and polishing with a diamond suspension up to 250 nm grain size. Such sections were observed and analysed using a scanning electron microscope Zeiss Evo 40, equipped with EDX detector PentaFET. The cathode contacting area of each sample was evaluated through image analysis (Fiji Imagej 1.47h) on SEM micrographs.

Results and discussion

Electrochemical characterization

The I-V curves of the cells measured at 750°C highlighted the strong influence of the contacting solution on the performances of the investigated system (figure 4). The cell electrically contacted at the cathode side only with platinum showed a power density of 423 $mWcm^{-2}$ at 0.7 V, a value by 30% lower than other state-of-art cells measured by other authors (8, 9). This power density is nevertheless comparable with results related to the same type of cells in stacks (18). The use of a shaped interconnect as cathodic current collector dramatically decreased the cell performances with a power density of 124 $mWcm^{-2}$ at 0.7 V. The fast voltage drop observed in this case was mainly caused by an excessive ohmic contribution as can be seen by the change in the slope of the voltage curve and confirmed by the impedance spectra (figure 5). The measured ohmic contribution was indeed 1.542 Ωcm^2, more than four times higher compared to the one measured on the previous cell contacted using platinum meshes (0.374 Ωcm^2). Consequently, the cell polarization suffered a performance decrease with the worsening of the total resistance, as it is visible in the impedance spectra by the increase of both the real resistive part and the imaginary capacitive contribution. In this case the real part value, calculated by the difference between the low-frequency and high-frequency intersections of the real axis by the impedance spectrum, increased from 0.520 Ωcm^2 to 0.743 Ωcm^2.

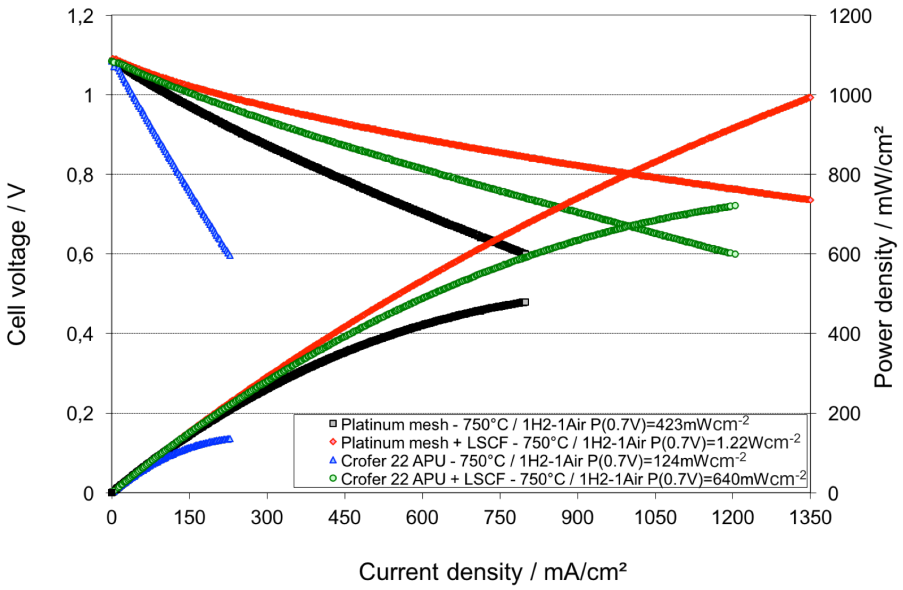

Figure 4. I-V curves and power densities of cells measured at 750°C, 1 Nl min^{-1} air at the cathode side and 1 Nl min^{-1} H_2 with 3 vol.%. H_2O at the anode.

The application of a LSCF contacting paste layer between the cathode and the current collector resulted in a beneficial effect for both platinum mesh and interconnect plate solutions. In the first case it was not possible to investigate the power output for the whole range of voltage from the open circuit voltage (OCV) down to 0.6 V because of current limitations of the testing device. The theoretical value of 1.22Wcm^{-2} at 0.7 V was however calculated by an extrapolation from intermediate values of the I-V curve. This corresponded to an improvement of 188% compared to the cell tested without contacting

material. Such improvement has been mainly related to the reduction of the ohmic contribution which value was 0.139 Ωcm^2 for this cell. Minor benefits were measured for the cell polarization, which decreased to a value of 0.463 Ωcm^2.

LSCF contacting paste applied between the cathode and the Crofer 22 APU interconnect led to intermediate performances (640 $mWcm^{-2}$ at 0.7V) between those of the abovementioned cells. Figure 5 shows that the use of a contacting layer made comparable the overall area specific resistance (ASR) of the cells despite the differences in the current collector geometries. The use of a metallic interconnect between the contacting layer and the Pt meshes resulted in a higher ohmic resistance (0.233 Ωcm^2) which was compensated by a lower polarization contribution (0.400 Ωcm^2). The comparison of such impedance results with the I-V curves highlighted the role of the ohmic losses in the overall cell performances since even for similar total ASR values the power density was affected by contacting issues to a greater extent as observed by Minh et al. (3).

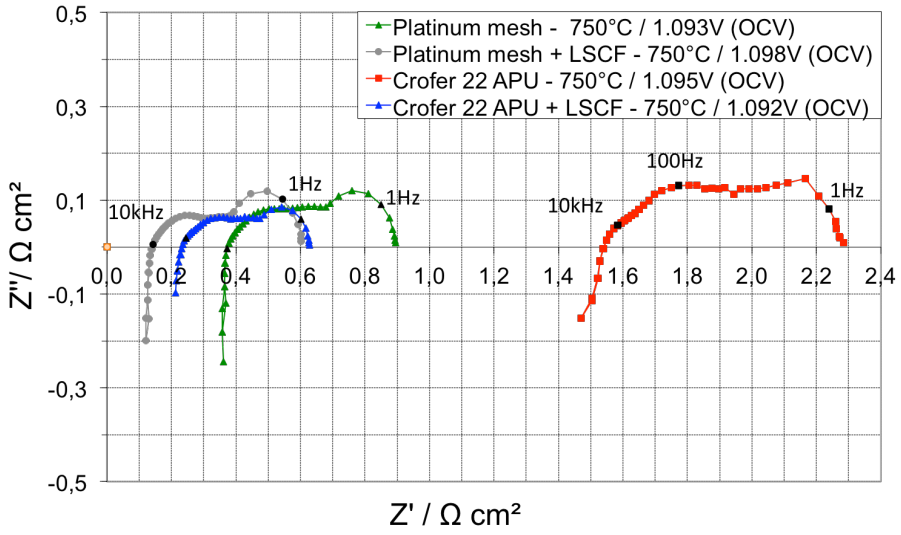

Figure 5. Impedance spectra of cells measured at OCV, 750°C, 1 Nl min^{-1} air at the cathode side and 1 Nl min^{-1} H_2 with 3 vol.%. H_2O at the anode.

Figure 6 reports the ohmic and polarization losses values of each tested cell together with the respective cathode/current collector contacting area. Without the application of the LSCF paste the different geometries resulted in similar contacting areas, 14% higher in the case of platinum meshes. The application of a contact layer emphasized the geometrical differences, mainly consisting in a different distribution of the contacting points. The embedding of the platinum mesh in the LSCF paste resulted in a 60% larger contact area compared to the use of the interconnect. The histograms highlight the inverse proportionality between the ohmic contribution and the extension of the contacting area. Such trend did not strictly occur for the polarization resistance. An inversion of it was observed for the cell tested with the contacting layer and platinum mesh as current collector. The main result arising from the collected data was that the usage of LSCF ink as contacting layer minimized the gap on the polarization values limiting the effect of the contacting area due to the current collector geometries.

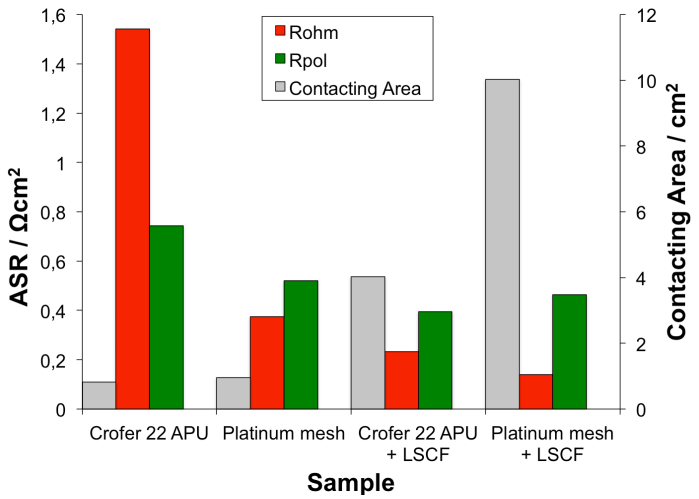

Figure 6. Ohmic, polarization losses and cathode contacting area.

Considering the strict relation between the contact area and the ohmic resistance contribution one can hypothesize their influence on the polarization losses as a matter of electric currents distribution.

Uneven currents over the cathode surface, due to a difference between the in-plane and cross-plane resistances (19), affect the electrode/current collector interface in a similar way to what happens in the electrode/electrolyte interface (20, 21). This results in the presence of cathodic sections where low or no current is flowing causing local inactivity of the electrode.

In Figure 7 the power densities of the cells measured at different voltages in function of their contacted area are shown. A threshold can be identified between 0.82 and 0.96 cm^2 above which the power density increases linearly with the amount of the cathode contacted area. The slope of such trend increases for lower cell potential, therefore for higher current densities. This makes relevant the importance of an improved current collection to ensure high cell performances exploiting large currents outputs. Below the identified threshold the insufficiency of contact points constitutes a bottleneck for the current collection resulting in limited cell performances and confirming the presence of inactive electrode portions.

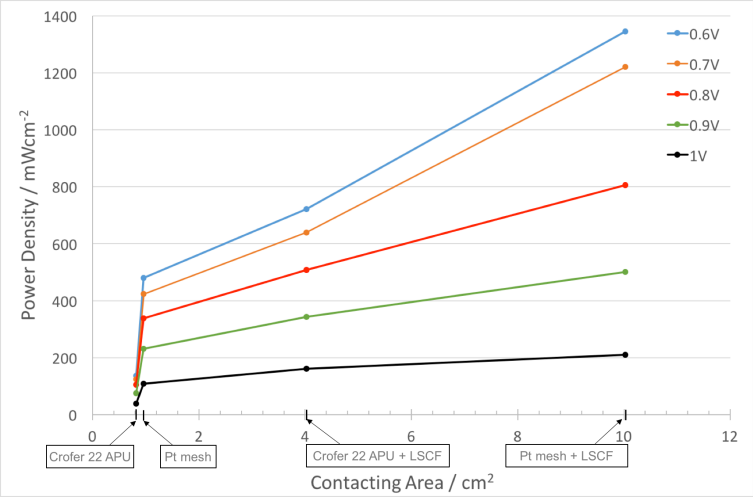

Figure 7. Influence of the cathode contacting area on the power density measured at different cell voltages.

To support these observations, the deconvolution of the impedance spectra was performed investigating the influence of the contacting solution on the processes occurring within the cell (Figure 8).

The contributions related to the anode functional layer, R_1 and R_2, were inversely proportional to the contacting area. The use of an interconnect as current collector without contacting paste resulted in the highest value of such contribution, three times larger compared with the use of platinum mesh. The addition of LSCF contacting paste minimized the gap between the values measured with different current collector geometries.

It was not possible to identify a clear trend also for the $R_{cathode}$ and R_{3anode} contributions. The cathodic resistance was influenced by the contacting area with the exception of the first value. The measured gas diffusion impedance of the anode was influenced by the contacting geometry showing lower values when the interconnect was used.

The correct identification of these contributions was however hampered by the strong overlapping of the processes at the intermediate frequencies which could lead to their improper quantification. Additionally, the impedance spectra recorded in the case of the cell contacted with the interconnect without LSCF paste presented a lower quality compared to the others (Figure 5). This feature can be due to the poor current distribution in such cell being its contact area below the threshold identified in Figure 7 and therefore affecting the AC signal. The low quality of the spectra affected the precision of the fitting results as can be observed by the error bars in Figure 8.

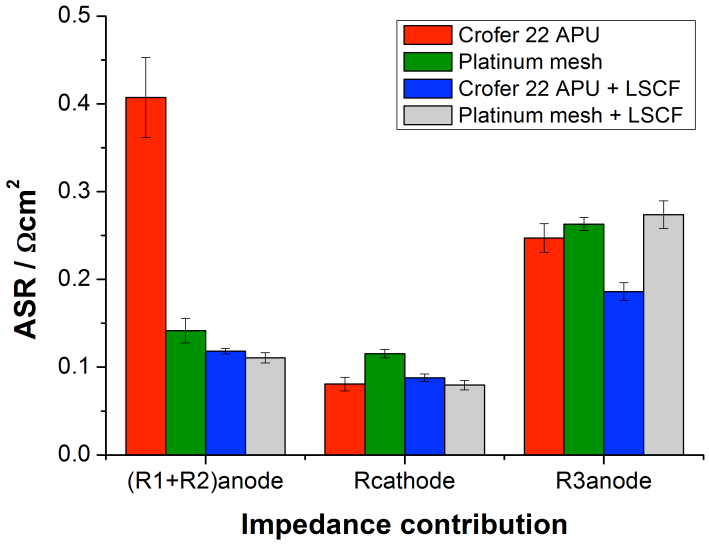

Figure 8. Impedance contributions calculated by CNRLS method.

Even if changes in the sample setup were made only at the cathodic compartment, a clear trend of related effects have been measured for the anode by EIS. Such behavior can be due to the higher anode lateral conductivity compared to the cathodic one and the mutual influence of the electrodes operation. Additionally, the anodic processes are of easier identification due to the range of frequencies at which they take place. The gap between the anodic functional layer impedance contributions, measured for the lower contacting area configurations, confirmed the threshold identified in Figure 7. High resistance values

can be due to the presence of inactive cell portions caused by poor current distribution originated by the cathodic contacting solution.

Post-experiment characterization

The post-experiment analyses revealed for all the tested cells a porous GDC barrier layer and the presence of strontium at the interface between it and the electrolyte (Figure 9). Such features, that could be linked together since strontium is able to migrate through the pores of the GDC layer, might be the cause of the lower measured performances compared to other state-of-art cells. The low density of the interlayer causes an increase of its resistance to the oxygen ions transport toward the electrolyte. Additionally, the reactivity of strontium with the YSZ of the electrolyte lead to the formation of low-conducting phases which are further detrimental for the system performances (22).

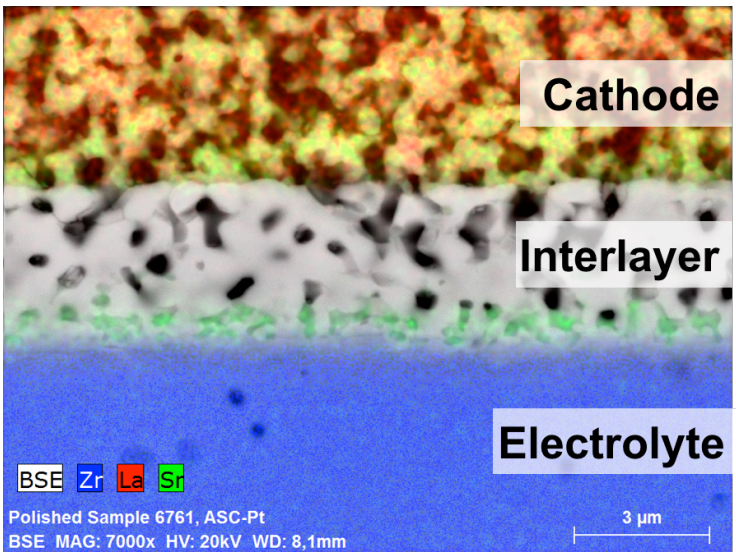

Figure 9. SEM-EDX map of the cross-section detail of the cathode/interlayer/electrolyte interfaces.

The cathodes showed inhomogeneous porosity in their section characterized by large pores far from the interlayer/cathode interface (Figure 1). High irregularities were found on top of the cathode layer which could be responsible of the limited electrical contact with the current collector. The use of a contacting paste ensured a larger exploitation of the cathode surface for the current distribution as observed by the electrical measurements.
In Figure 10 the complete section of an ASC is shown including the contacting LSCF. This layer resulted well adherent to the cathode even after the cross section preparation. The discontinuity in the contacting layer is due to the footprint of the interconnect.

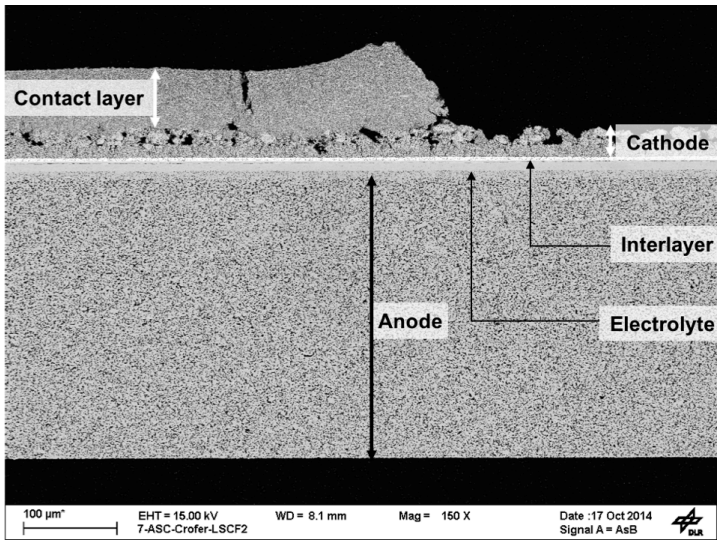

Figure 10. SEM-BSE image of the cross-section of an ASC with the LSCF contact layer on the cathode.

Conclusions

In this work ASCs have been tested with different cathodic contacting solutions in terms of geometry and of the application of LSCF ink as contacting layer between the electrode and the current collector. The measured cell performances by means of I-V curves and EIS highlighted the influence of the ohmic losses on the cell polarization and the direct effect on the power output.

The ohmic resistance contribution to the measured impedance showed an inverse proportionality to the extension of the cathode contacted area, while the cell polarization resulted influenced to a minor extent. However, the deconvolution of the impedance spectra evidenced that among the contributions to the cell polarization, processes related to the anodic functional layer were strongly affected by the changes in the contacting solutions. This result confirms the presence of inactive portions of the cell, identified by the impedance spectra. A reduced activity of the anode was measured as a consequence of the poor current distribution along the cell in case of reduced extension of the cathode contacting area.

The results of this work evidenced the need of a suitable contacting solution not only when cells are introduced in a stack but during laboratory tests of cells as well. To compare the performances of cells is indeed necessary to eliminate the variable of the contacting area by fixing the related parameters and solutions. The closer the contacting solution to the real stack the higher the meaning of the measured cell's performance will be. The effects on the current distribution influence the quality of the impedance spectra and the cell processes to a different extent jeopardizing their comparison.

From the practical point of view, a larger influence on the cell power output of the ohmic resistance contribution was observed compared to the polarization resistance. This evidenced the need to maximize the current collection acting on the cathode contacting in order to improve cell performances exploitation.

Acknowledgments

The authors would like to acknowledge I. Plock, G. Steinhilber and O. Freitag for the technical support. The research leading to these results has received funding from the European Union's Seventh Framework Programme (FP7/2007-2013) Fuel Cells and Hydrogen Joint Undertaking (FCH-JU-2013-1) under grant agreement No 621207.

References

1. S. P. Jiang, *J. Electrochem. Soc.*, 148(8), A887 (2001)
2. Nguyen Q. Minh, Mogens B. Mogensen, Interface, 22, 4 (winter 2013)
3.Nguyen Q. Minh, Abhijith Budur, Fatih Dogan, ECS Transactions, 68, 2273 (2015)
4. Z. Lu, J. Hardy, J. Templeton, J. Stevenson, *Journal of Power Sources,* 196, 39 (2011)
5. S.P. Jiang, J.G. Love, L. Apateanu, *Solid State Ionics*, 160, 15 (2003)
6. M. C. Tucker, L. Cheng, L.C. DeJonghe, *Journal of Power Sources*, 196, 8313 (2011)
7. V.A.C. Haanappel, N. Jordan, A. Mai, J. Mertens, J.M. Serra, F. Tietz, S. Uhlenbruck, I.C. Vinke, M.J. Smith, L.G.J. de Haart, *J. Fuel Cell Sci. Technol* 6(2), 021302 (2009)
8. V.A.C. Haanappel, A. Mai, J. Mertens, *Solid State Ionics,* 177, 2033 (2006)
9. V.A.C. Haanappel, M.J. Smith, *Journal of Power Sources*, 171, 169 (2007)
10. A. Leonide, S. Hansmann, A. Weber, E. Ivers-Tiffée, Journal of Power Sources 196 (2011) 7343
11. C. Endler-Schuck, A. Leonide, A. Weber, S. Uhlenbruck, F. Tietz, E. Ivers-Tiffée, Journal of Power Sources 196, 7257 (2011)
12. M. Kornely, A. Neumann, N.H. Menzler, A. Leonide, A. Weber, E.Ivers-Tiffée, J. of Power Sources 196, 7203 (2011)
13. A. Leonide, V. Sonn, A. Weber, E. Ivers-Tiffée, *J. of Electrochem. Soc*. 155, B36 (2008)
14. B.A. Boukamp, Solid State Ionics, 20, 31 (1986)
15. J.R. Macdonald, L.D. Potter, Solid State Ionics, 24, 61 (1987)
16. D.W.Marquardt, J. Soc. Ind. Appl. Math. 11, 431 (1963)
17. K. Levenberg, Q. Appl. Math. 2, 164 (1944)
18. C. Comminges, Q.X. Fu, M. Zahid, N. Y. Steiner, O. Bucheli*, Electrochimica Acta,* 59, 367 (2012)
19. F.H. van Heuveln, H.J.M. Bouwmeester, F.P.F. van Berkel, *J. Electrochem. Soc.,*144, 126 (1997)
20. J.Fleig, J. Maier, *J. Electrochem. Soc*., 144, L302 (1997)
21. A. C. S. Sabioni, A. N. Huntz, F. Millot, C. Monty, *Philos. Mag. A*, 66, 361 (1992)
22. H.-G. Jung, Y.-K. Sun, H. Y. Jung, J.S. Park, H.-R. Kim, G.-H. Kim, H.-W. Lee, J.-H. Lee, *Solid State Ionics*, 179, 1535 (2008)